doi:10.1111/evo.14519

Genome size drives morphological evolution in organ-specific ways

Michael W. Itgen,[1,2] Giovanna R. Natalie,[3] Dustin S. Siegel,[4] Stanley K. Sessions,[3] and Rachel Lockridge Mueller[1,5]

[1]*Department of Biology, Colorado State University, Fort Collins, Colorado 80523, USA*

[2]*E-mail: Itgenm@colostate.edu*

[3]*Biology Department, Hartwick College, Oneonta, New York 13820, USA*

[4]*Department of Biology, Southeast Missouri State University, Cape Girardeau, Missouri 63701, USA*

[5]*E-mail: rachel.mueller@colostate.edu*

Received August 19, 2021

Accepted April 11, 2022

Morphogenesis is an emergent property of biochemical and cellular interactions during development. Genome size and the correlated trait of cell size can influence these interactions through effects on developmental rate and tissue geometry, ultimately driving the evolution of morphology. We tested whether variation in genome and body size is related to morphological variation in the heart and liver using nine species of the salamander genus *Plethodon* (genome sizes 29–67 gigabases). Our results show that overall organ size is a function of body size, whereas tissue structure changes dramatically with evolutionary increases in genome size. In the heart, increased genome size is correlated with a reduction of myocardia in the ventricle, yielding proportionally less force-producing mass and greater intertrabecular space. In the liver, increased genome size is correlated with fewer and larger vascular structures, positioning hepatocytes farther from the circulatory vessels that transport key metabolites. Although these structural changes should have obvious impacts on organ function, their effects on organismal performance and fitness may be negligible because low metabolic rates in salamanders relax selective pressure on function of key metabolic organs. Overall, this study suggests large genome and cell size influence the developmental systems involved in heart and liver morphogenesis.

KEY WORDS: Cell size, comparative methods, evolutionary development, histology, microCT, salamanders.

The evolutionary trajectories of morphological traits reflect lineages' intrinsic capacities to generate novel phenotypes and selection to match these phenotypes to the environment. Although optimal trait values theoretically exist for any organism in any environment, in reality, the number of possible phenotypes is biased by limitations introduced at all levels of biology (Maynard Smith et al., 1985; Arnold, 1992; Brakefield, 2006; Gerber, 2014). Possible phenotypes can be delineated in morphospace from merely theoretical ones by whether the phenotypes can be produced by a species' developmental system (Alberch, 1982; Salazar-Ciudad, 2006). The process of development is an emergent property of biochemical and cellular interactions that direct morphogenesis. Morphogenesis as a process involves dynamic changes in gene expression and signal transduction networks that instruct populations of cells to divide, differentiate, migrate, and coalesce (Alberch, 1982; Oster et al., 1988; Chan et al., 2017; Maroudas-Sacks and Keren, 2021). In addition, cells influence their neighbors, relaying positional and deterministic information to one another that results in the induction of tissue formation and organogenesis. When genes, proteins, or cells evolve within this system, any new variant can potentially alter these collective interactions and change the outcome of development.

Alberch (1982) proposed that the primary forces underlying the evolution of morphology are changes to the biochemical and cellular interactions involved in development. Overall, development is robust to change, and variation—both mutational and epigenetic—can often have no impact on the resulting phenotype (Lewontin, 1972; Oster and Alberch, 1982; Wagner, 2011; Uller et al., 2018). However, some changes will result in the developmental system producing a different phenotype (Oster and Alberch, 1982; Uller et al., 2018). These changes cross a theoretical threshold called a bifurcation boundary, which bounds the

amount of variation permittable within a developmental system that still produces the same outcome (Oster and Alberch, 1982). This variation can exist in many parameters, including sequence, structure, function, and interaction of genes and proteins; rates of diffusion and biochemical reactions; morphology and motility of cells; rates of cellular division and differentiation; and the size and organization of tissues and structures (Alberch, 1983; Brakefield et al., 2003; Mallarino et al., 2011; Keyte and Smith, 2014; Powder et al., 2015). Variation in these parameters can alter morphogenesis and result in larger scale changes that impact the rate of development, the sequential timing of developmental events, or pattern formation, ultimately producing novel phenotypes (Oster and Alberch, 1982).

Genome size is a trait that can directly impact developmental systems through its effects on cell biology (Gregory, 2005). There is a strong positive correlation between genome size and cell size, resulting in cells becoming larger as DNA accumulates (Gregory, 2005; D'Ario et al., 2021). Large cell size has clear impacts on cell morphology, shifting the ratio between surface area and volume and causing the scaling of intracellular organelles (Marshall et al., 2012). Genome and cell size together have been shown to impact developmental systems through two mechanisms (Gregory, 2005). First, large genome and cell sizes slow developmental rate by causing longer cell cycles and slower rates of cell migration and differentiation (Sessions and Larson, 1987; Schmidt and Roth, 1993; Vinogradov, 1999). This slowing can ultimately shift the timing of developmental events (i.e., lead to heterochrony) and impact the dynamics of morphogenesis (Alberch et al., 1979; Gould, 1985). Changes in cell size also impact the final outcomes of development: the structures of tissues and organs (Alberch and Alberch, 1981; Hanken and Wake, 1993; Roth et al., 1993). Evolutionary increases in genome and cell size can result in organs and organisms that are composed of fewer, larger cells, assuming body size and organ size remain constant (Hanken and Wake, 1993). Morphogenesis must then emerge from interactions among fewer, larger cells. Extensive work in *Drosophila*, as well as mammalian model systems, has shown the Hippo pathway to be the master regulator of organ size, serving as a hub to integrate information from numerous signaling pathways that are active during development. This network produces morphogen gradients that define organ size, with cells within the field specified by the gradient growing, proliferating, and undergoing apoptosis in response to genetic and mechanical cues to achieve the target size (Gokhale and Shingleton, 2015; Kim and Jho, 2018). Thus, increasing cell size must be accommodated by this conserved network to achieve final organ sizes proportionate to body size. Additionally, the final tissue or organ must maintain structure and function with fewer, larger cells. To highlight the importance of this interaction between cell size and body size, Hanken and Wake (1993) introduced the concept of biological size—a proxy for the number of cells comprising an organism—rooted in empirical observations of how morphology changes when organisms evolve to be composed of few large cells (Hanken, 1982, 1983; Linke et al., 1986; Roth et al., 1988, 1990, 1993, 1994).

Empirical studies of morphological evolution have suggested that the impacts of increased genome and cell size—mediated through alterations to the developmental system—can vary extensively across different tissues, organs, and species (Fankhauser, 1945; Hanken and Wake, 1993; Roth et al., 1993; Snyder and Sheafor, 1999; Womack et al., 2019). Amphibians, particularly salamanders, have provided a powerful system for studying these patterns and processes due to their enormous range in genome (9.3–120 gigabases [Gb]) and cell size (Horner and Macgregor, 1983; Gregory, 2005; Sessions, 2008; Decena-Segarra et al., 2020; Sessions and Wake, 2021). Much of this work has focused on the brain and nervous system, the skeletal system, and the circulatory system. For example, within the salamander brain, dramatic changes in gross morphology and tissue organization are connected to larger genome and cell sizes as well as reductions in cell numbers (Roth et al., 1993; Roth and Walkowiak, 2015). Similarly, repeated loss and reduction of skeletal elements have been observed across amphibians resulting from reductions in cell number or slower developmental rates associated with large genome and cell sizes (Alberch and Alberch, 1981; Hanken and Wake, 1993; Womack et al., 2019). In tropical lungless salamanders with exceptionally large genomes, the associated slower development rates appear to be connected to paedomorphic morphologies including fenestrated skulls, highly reduced or even absent phalangeal elements in the digits, and extensively webbed feet (Wake, 1966; Alberch and Alberch, 1981; Alberch, 1983; Jaekel and Wake, 2007; Decena-Segarra et al., 2020).

The diversity of morphological outcomes in the studies carried out to date suggests that the fundamental rules governing the effects of genome and cell size on morphological evolution will be revealed through the analysis of additional organs and the synthesis of results across species and organ systems. As a step toward this goal, our study investigates how increases in genome and cell size impact the morphology of the heart and liver. These two previously unexplored organs differ in morphogenesis and function; the heart has a kinetic biomechanical function and the liver has a biochemical and secretory function. However, the organs are similar in that both serve key functional metabolic roles for the organism. Salamanders have incredibly low metabolic rates that appear unrelated to genome and cell size (Gatten et al., 1992; Uyeda et al., 2017; Gardner et al., 2020; Johnson et al., 2021). Thus, the salamander heart is circulating blood in an organism with the lowest O_2 requirements among terrestrial vertebrates. Low metabolic rates also decrease the demand for the

liver to metabolize macromolecules (i.e., carbohydrates, lipids, proteins) needed for oxidative phosphorylation and glycolysis. We hypothesize that the extremely low metabolic rates of salamanders relax selection on heart and liver function. This relaxed selection, in turn, allows for a larger number of functionally adequate morphologies—a relatively flat adaptive landscape—with organ phenotype free to evolve driven by changes in genome size.

Our study system is the lungless salamander genus *Plethodon*, which includes species with a broad range of genome sizes (23–67 Gb) and cell sizes shaped by stochastic evolutionary processes, but uniformity or lower diversity in potentially confounding variables (e.g., life history, body size) that could also impact organ structure and function (Highton, 1995; Newman et al., 2016; Mueller et al., 2021). Using diffusible iodine-based contrast-enhanced computed tomography (diceCT) and histology applied to nine focal *Plethodon* species, we quantified metric body size, organ size, and several measures of tissue composition and geometry: (1) proportion of the heart wall composed of cardiomyocytes versus intertrabecular space (i.e., lacunae), (2) proportion of the liver composed of hepatocytes versus vascular openings, and (3) the numbers and sizes of distinct vascular structures (sinusoids, veins, arteries) in the liver. We used phylogenetic comparative methods to test whether these variables correlate with evolutionary changes in genome and cell size. Based on our findings, we propose hypotheses connecting cell size, developmental system perturbation, and morphology. More generally, we discuss how relaxed demands on organ function can allow the evolution of a range of structurally different morphologies.

Methods

ANIMAL COLLECTION

We collected five adult individuals of *P. cinereus*, *P. cylindraceus*, *P. dunni*, *P. glutinosus*, *P. idahoensis*, *P. metcalfi*, *P. montanus*, *P. vandykei*, and *P. vehiculum*. Permit IDs and locality data can be found in the Supporting Information. Salamanders were collected and euthanized in neutral buffered (pH 7) 1% MS-222, fixed in buffered formalin, and transferred through a graded series of ethanol (10%, 30%, 50%, 70%) before storage in 70% ethanol. Due to the rarity of some species included in this study, we used the same specimens for the diceCT and histological analyses. The protocols for animal research, husbandry, and euthanasia were approved by the Institutional Animal Care and Use Committee.

diceCT DATA GENERATION AND PROCESSING

We used diceCT to measure liver and heart volumes (Gignac et al., 2016). I_2KI staining can cause varying degrees of tissue shrinkage, but these artifacts can be minimized by using low concentrations of I_2KI and shorter staining periods (Baverstock et al., 2013; Vickerton et al., 2013; Hedrick et al., 2018). To minimize such shrinkage, we used a 1% I_2KI solution and incubated the specimens for 2 days, which was shown to produce the smallest degree of tissue shrinkage (Vickerton et al., 2013). After scanning, the I_2KI was rinsed out using several changes of 70% ethanol and specimens were stored in 70% ethanol. In addition, all specimens were treated uniformly to minimize the risk of any potential I_2KI-related artifacts or shrinkage introducing noise or bias into subsequent histological analyses. Following these precautions, we did not observe any significant signs of tissue shrinkage across organs and specimens.

Specimens were scanned twice using a Bruker SkyScan 1173 at the Karel F. Liem Bioimaging Center, Friday Harbor Laboratories, University of Washington. Scans were set to 85 kV and 90 μA with a 1-mm aluminum filter to reduce beam hardening. We first produced full body scans to measure liver volumes at a resolution ranging from 14.9 to 17 μm, depending on the size of the specimens. We then produced higher resolution scans for the heart, which were scanned at a resolution ranging from 7.1 to 9.9 μm. diceCT scans were reconstructed using NRecon (Bruker, 2005–2011) following standard operating procedures including optimal *x*/*y* alignment, ring artifact reduction, beam hardening correction, and a post-alignment. Data visualization and analysis were accomplished using 3DSlicer (Fedorov et al., 2012). Liver and heart ventricle volumes were calculated through segmentation of the liver and heart from each specimen.

ORGAN MEASUREMENT

Snout-vent lengths were measured to the nearest 0.01 mm for each individual using digital calipers. The hearts and livers were then excised from specimens and were embedded in plastic following standard protocols (Humason, 1962). Tissues were sectioned at 4 μm and stained with hematoxylin for 4 min and toluidine for 3 min. Sections were mounted and then visualized using a compound microscope. Images used in the analysis were minimally edited to remove blood cells that obstructed vascular structures or the intertrabecular space of the ventricular myocardium. Five images were taken (one each from five different histological sections) at 20× magnification for each individual and a mean value was calculated for each morphological trait per individual. We decided to collect morphological data from five images after finding no significant differences when the data were collected from three, five, or 10 images. Each image was converted to grayscale and a thresholding method was used to collect the morphometric data. ImageJ was used for all image processing and analysis (Schneider et al., 2012).

Amphibian livers are primarily composed of hepatic tissue that is permeated by the vasculature (Akiyoshi and Inoue, 2012). Liver vascular structures consist of hepatic arteries that provide oxygen, portal veins that bring nutrients and toxins to the liver,

and sinusoids, which are specialized capillaries where oxygen-rich blood from hepatic arteries and nutrient-rich blood from portal veins mix (Elias and Bengelsdorf, 1952). Liver tissue is generally arranged into many hepatic lobules that are centered by portal triads—an arrangement of hepatic arteries, portal veins, and bile ducts (Elias and Bengelsdorf, 1952). The network of sinusoids gives the hepatic tissue a cord-like appearance in most vertebrate taxa, with hepatocytes forming cords that are one- to two-cell thick; this morphology increases the surface area of each hepatocyte that is in contact with circulating blood (Elias and Bengelsdorf, 1952). However, some species of salamanders have a many-cell thick arrangement of hepatic cords (Akiyoshi and Inoue, 2012). For the liver, we measured the total area of each histological section that was composed of tissue (primarily hepatocytes) versus vascular openings and the number and size of distinct vasculature (sinusoids, veins, arteries) (Fig. S1). Twenty nuclei and cells were also measured for each individual to collect data on hepatocyte nuclear and cell area.

Amphibians have a single, thin-walled ventricle that has a central chamber surrounded by a highly trabeculated network of myocardium, which is a characteristic of ectotherms (Stephenson et al., 2017). Heart morphology in *Plethodon* also reflects the lack of lungs in the family Plethodontidae, which has been accompanied by a loss of complete atrial septation (Lewis and Hanken, 2017). For the heart ventricles, we measured the myocardial area in the ventricle walls versus intertrabecular space in each histological section (Fig. S1). We focused on this because the trabeculated myocardium makes it difficult to define the edges of the ventricle chamber. We did not measure any characteristics of the atria because they lack distinct internal structure and their elastic nature made accurate volumetric measurements impossible.

GENOME SIZE MEASUREMENT

Genome size was measured using the Feulgen-staining method on fixed erythrocytes following the protocol of Sessions and Larson (1987). *Ambystoma mexicanum* (32 Gb) was used as a standard to calculate the genome sizes of the other species. The *A. mexicanum* were acquired from the *Ambystoma* Genetic Stock Center at the University of Kentucky. Erythrocytes were extracted from the *Plethodon* and *Ambystoma* specimens fixed in neutral-buffered (pH 7) formalin, and transferred to microscope slides to produce blood smears. We collected blood smears from three to five individuals per species. The cells were hydrated for 3 min in distilled water, permeabilized in 5 N HCl for 20 min at 20°C, and then rinsed three times in distilled water. Nuclei were stained with Schiff's reagent for 90 min at 20°C, destained in 0.5% sodium metabisulfite three times for 5 min each, and then rinsed in distilled water three times. The stained cells were dehydrated in a graded series of 70%, 95%, and 100% ethanol, dried, and mounted. Each staining run included a slide of *Ambystoma* cells as the standard. We photographed 2–12 ($\bar{x} = 5.5$) nuclei per individual under 100×, and the integrated optical densities (IOD) were measured using IMAGE PRO software (Media Cybernetics, Rockville, MD, USA). Genome sizes were calculated by comparing the average IODs of the experimental species to the IOD of the standard. Nuclear areas were measured for each erythrocyte using IMAGE PRO software, and hepatocyte nuclear and cell areas were also calculated for 20 cells from each of four to five individuals using IMAGE PRO. We tested for the predicted correlations between genome size and nuclear area and cell area using linear regression.

PHYLOGENY

We estimated the phylogenetic relationships among the nine species of *Plethodon* used in this study to account for phylogenetic nonindependence in our analyses. DNA sequences for the mtDNA gene cytb and the nuclear gene Rag1 were obtained from NCBI (https://www.ncbi.nlm.nih.gov/genbank; Table S1). The cytb and Rag1 sequences were aligned independently using MUSCLE in MEGA version 7 with default parameters and trimmed to 629 and 1467 base pairs, respectively (Edgar, 2004; Kumar et al., 2016). We applied a codon-specific nucleotide substitution model determined by the best-fit models using AICc with PartitionFinder 2 using the "greedy" search algorithm (Lanfear et al., 2017). We applied the following model scheme: Rag1 codon position 1, F81; Rag1 codon position 2, HKY + I; Rag1 codon position 3, HKY; cytb codon positions 1–2, GTR + G; and cytb codon position 3, HKY + G. The phylogeny was estimated using Bayesian inference with MrBayes version 3.2.5 (Ronquist et al., 2012). The analysis ran with four chains (three heated and one cold) for 10 million generations with sampling occurring every 1000 and the first 10% of the sampled trees discarded as burnin.

DATA ANALYSIS

We log-transformed all variables to account for nonnormal distributions and created phylogenetic generalized least squares (PGLS) models that simultaneously estimated Pagel's lambda (λ), a measure of phylogenetic signal (Revell, 2010). Each PGLS model included one of the morphological traits as a response and genome size and SVL as the predictor variables to test if organ morphology is correlated with genome size and/or SVL while accounting for phylogeny. For each species, we also calculated the biological size index (BSI)—a relative measure of the total number of cells comprising an organism that is based on organism size and cell size—by dividing the mean SVL by the square-root of genome size (Hanken and Wake, 1993; Decena-Segarra et al., 2020). Our response variables were liver size, ventricle size, total area composed of muscle in the ventricle, number of vascular structures in the liver, average size of the vascular

structures in the liver, and the total area composed of hepatic tissues in the liver. The PGLS analyses were conducted using R version 3.4.2 and the packages *caper* and *nlme* (Orne et al., 2013; R core team, 2016; Pinheiro et al., 2021). We applied a Brownian motion model of evolution to all variables, and we applied a Benjamini-Hochberg false discovery rate correction to account for multiple testing (Benjamini and Hochberg, 2000). We visualized the magnitude and direction of changes in genome size across the nine species of *Plethodon* in the study using the contMap function in the R package *phytools* on the estimated topology (Revell, 2012).

Results

The genome size measurements for the nine *Plethodon* species ranged from 29.3 to 67.0 Gb (Fig. 1; Table 1). The genome sizes measured in this study were generally larger than those previously published or fell within the higher range of published measurements (Gregory, 2021). We measured larger genome sizes for *P. cinereus* (29.3 vs. 25.6 Gb, the mean of previously published measurements), *P. dunni* (52.3 Gb vs. previously published mean = 46.5 Gb), and *P. vehiculum* (46.4 Gb vs. previously published mean = 39.1 Gb). Our genome size measurement for *P. glutinosus* was comparable to the higher published measurement for the species (38.9 vs. 42.1 Gb; Bachmann, 1970) but is much larger than the average published value for this species (mean = 28.0 Gb). We also found that *P. idahoensis* has the largest genome size in the genus at 67.0 Gb (Gregory, 2021). Conversely, we measured a significantly smaller genome size for *P. vandykei* (54.6 vs. 67.8 Gb; Mizuno and Macgregor, 1974), which was previously considered to have the largest genome size in the genus. Intraspecific variation in genome size measurements could, in principle, reflect true variation within and among populations, changes in taxonomic assignments (i.e., *P. glutinosus* complex; Highton, 1989), and/or technical discrepancies across studies (Hardie et al., 2002). We circumvented these sources of uncertainty by collecting our own genome size data on the same organisms we used for morphological analysis. The areas of nuclei from both hepatocytes ($R^2 = 0.955$; $P < 0.001$) and erythrocytes ($R^2 = 0.935$; $P < 0.001$) as well as hepatocyte cell area ($R^2 = 0.915$; $P < 0.001$) all have a significant positive correlation with these genome size measurements (Fig. 4; Table 1). Although these correlations do not verify the accuracy of our measurements of absolute genome sizes, they do provide confidence in the accuracy of their relative sizes, which is the most important feature of the dataset for our downstream analyses.

Morphological and histological trait data are summarized in Table 2. Mean SVL ranged from 40.1 mm in *P. cinereus* to 68.7 mm in *P. dunni*. Mean ventricle volume spanned an order of magnitude across this range of body sizes—from 0.52 mm^3 in *P. cinereus* to 5.72 mm^3 in *P. dunni*. Mean liver volume showed a nearly sevenfold range across these body sizes, from 15.9 mm^3 in *P. cinereus* to 112.1 mm^3 in *P. dunni*. Mean myocardial density showed a nearly threefold range across species, from 0.04 mm^2 per section in *P. idahoensis* to 0.118 mm^2 per section in *P. cinereus*. The mean number of vascular structures in the liver showed a ~2.5-fold range, from 23.5 per section in *P. idahoensis* to 60.0 in *P. cinereus*. Mean size of vascular structures showed a nearly three-fold range, from 0.0021 mm^2 in *P. cylindraceus* and *P. glutinosus* to 0.0061 mm^2 in *P. idahoensis*. Mean hepatic tissue area showed the smallest range across species, from 0.127 mm^2 in *P. glutinosus* to 0.143 mm^2 in *P. idahoensis*.

The results from the PGLS analyses are presented in Table 3. In the heart, genome size was negatively correlated with myocardial area in the ventricle ($P = 0.001$; Figs. 2, 6). In the liver, genome size showed both positive and negative correlations with different traits: genome size was positively correlated with the average size of the vascular structures ($P < 0.001$; Figs. 3, 6) but negatively correlated with the number of vascular structures ($P < 0.001$; Figs. 3, 6). In addition, genome size was positively correlated with the total hepatic tissue area ($P = 0.005$; Figs. 3, 6).

Body size (SVL) was positively correlated with ventricle size ($P < 0.001$) and liver size ($P < 0.001$; Figs. 5, S2). There were also significant positive correlations between body size (SVL) and the total hepatic tissue area ($P = 0.004$), the average vascular structure size in the liver ($P = 0.004$), and the number of vascular structures in the liver ($P = 0.012$). Thus, these three liver traits—hepatic tissue area, average size of the vascular structures, and the number of vascular structures—were significantly correlated with both genome size and SVL. We also plotted BSI and each of these traits to allow visualization of the relationships among them (Fig. 7).

Discussion

BODY SIZE, BIOLOGICAL SIZE, AND HEART AND LIVER MORPHOLOGY

The size of an organism or organ is a function of cell size and cell number. We found that ventricle and liver sizes were positively correlated with body size but not genome size in *Plethodon* salamanders, indicating that the size of these organs is a function of body size (Figs. 5, S2). Overall, we found no relationship between genome size and body size in *Plethodon*, indicating that increases in cell size do not produce larger body sizes. Thus, the evolution of larger genome and cell size in *Plethodon* is accompanied by a reduction in total cell numbers (i.e., reduced biological size) for both the ventricle and liver. Three variables—hepatic area, and number and size of vascular structures in the liver—were correlated with both body size and genome size. For the number and size of liver vascular structures, genome size

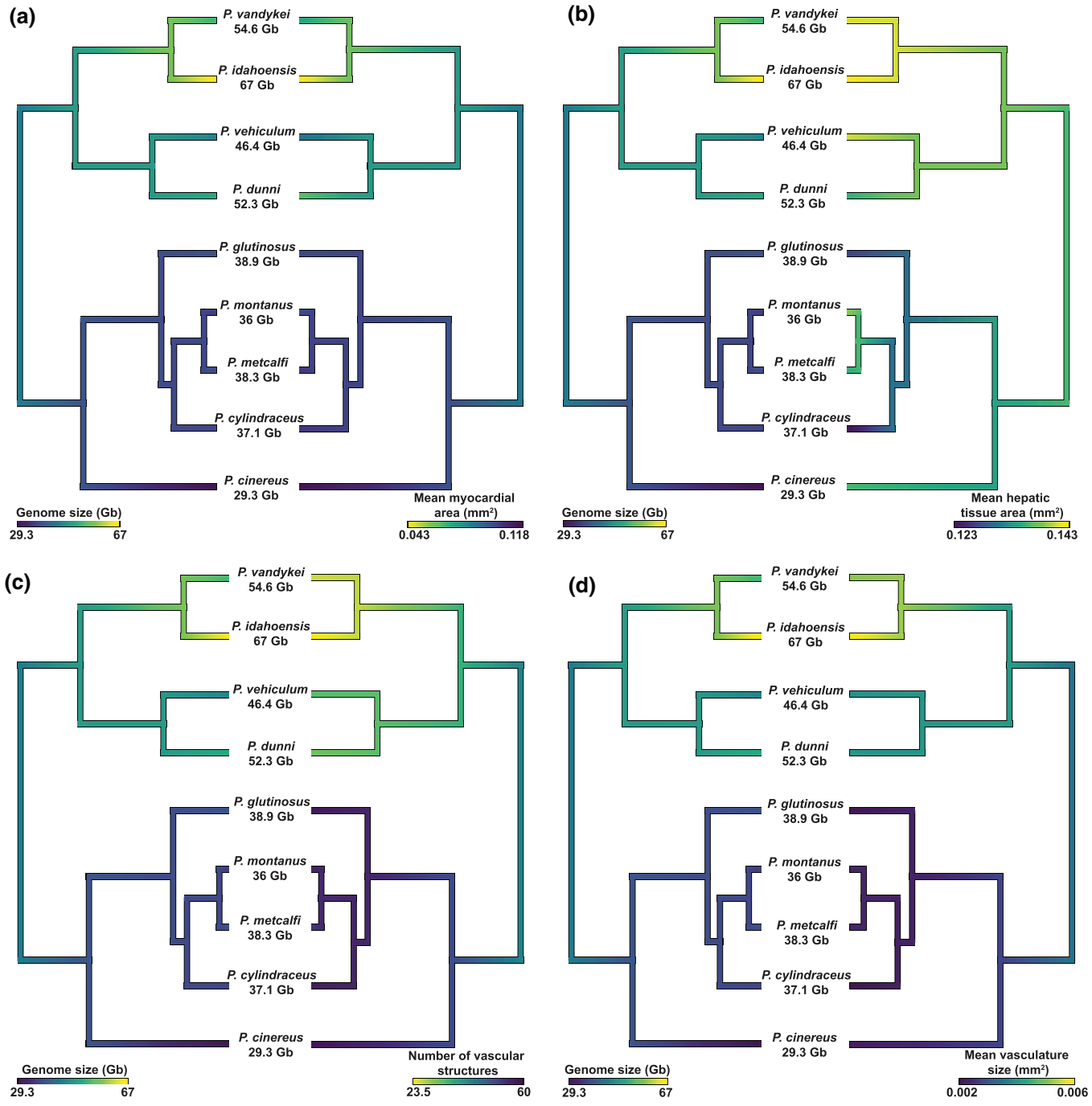

Figure 1. **Trait-mapped phylograms to visualize the coevolution of genome size and (a) mean myocardial area in the ventricle, (b) mean hepatic tissue area, (c) number of vascular structures in hepatic tissue sections, and (d) the mean size of vascular structures in hepatic tissues among the nine species of *Plethodon*.**

appeared to be a stronger predictor than BSI, suggesting that it is cell size itself—more so than cell size relative to organ size—that underlies changes in morphology (compare Fig. 6c,d with Fig. 7b,c). Similarly, myocardial area was correlated only with genome size, again suggesting that it is cell size itself that underlies changes in morphology. Only hepatic tissue area was better explained by BSI than cell size.

ORGAN MORPHOLOGY CORRELATES WITH GENOME AND CELL SIZE IN THE HEART AND LIVER AS WELL AS IN OTHER BODY SYSTEMS

The heart and liver each showed a distinct pattern of phenotypic change accompanying evolutionary increases in genome and cell size in *Plethodon*. In the heart, large genome and cell size were accompanied by a dramatic reduction in the amount of

Table 1. **Mean and standard deviation for measurements of genome size, nuclear areas of erythrocytes and hepatocytes, and cell areas of hepatocytes. $n = 5$ individuals unless otherwise noted; three to five erythrocyte nuclei and 20 hepatic nuclei and cells were measured per individual.**

Species	Genome Size (Gb)	Nuclear Area of Erythrocytes (μm^2)	Nuclear Area of Hepatocytes (μm^2)	Cell Area of Hepatocytes (μm^2)
Plethodon cinereus	29.3 ± 1.34 (n = 4)	54.5 ± 3.6	84.2 ± 3.7	373.8 ± 59.5
P. montanus	36.0 ± 3.4	58.7 ± 5.1	92.5 ± 4.6	515.3 ± 34.8
P. cylindraceus	37.1 ± 5.4	66.9 ± 10.4	92.2 ± 3.9	550.4 ± 27.2
P. metcalfi	38.3 ± 1.04	58.5 ± 2	87.7 ± 3.8	492.7 ± 90.3
P. glutinosus	38.9 ± 3.94	62.5 ± 6.2	97.8 ± 6.4	498.6 ± 42.9
P. vehiculum	46.4 ± 7.08 ($n = 3$)	86.4 ± 17.6	128.8 ± 5.6	740.1 ± 71.4
P. dunni	52.3 ± 4.06	88.2 ± 5.7	137.1 ± 6.2	755.2 ± 108.6
P. vandykei	54.6 ± 2.2 ($n = 4$)	104.3 ± 20.4	158.4 ± 9.8	943 ± 227.5
P. idahoensis	67.0 ± 2.31	116.9 ± 2.9	181.7 ± 8	984.5 ± 371

trabeculated myocardia relative to the intertrabecular space. Because ventricle size was not correlated with genome and cell size, the reduced myocardial density in species with large genome sizes resulted in hearts with relatively fewer myocardial cells overall.

In the liver, the vascular structures were most significantly impacted by genome and cell size, which resulted in distinct changes to tissue geometry. The average area of the vascular structures, which included hepatic arteries, portal veins, and sinusoids, was positively correlated with genome size. Conversely, the total number of these vascular structures was negatively correlated with genome size. Thus, livers in species with the largest genome sizes had significantly fewer, but larger, vascular structures. These results suggest that arteries, veins, and liver sinusoids increase in size to accommodate larger blood cells, which in turn changes the geometry and composition of liver tissue (Snyder and Sheafor, 1999). The changes in tissue geometry and composition resulted in two dramatic alterations to overall hepatic morphology. First, the arrangement of vascular structures into a portal triad-like organization was uncommon and became increasingly rare as genome and cell size increased. Although the hepatic arteries, portal veins, and bile ducts were present, they were rarely arranged together in a canonical portal triad. Second, the hepatocytes lacked the one- to two-cell-thick, cord-like morphology, which resulted in numerous hepatocytes having no direct contact with circulating blood. Akiyoshi and Inoue (2012) and others described this same several-cell-thick plate morphology in salamanders (Akat and Göçmen, 2014; Akat and Arkan, 2017; Vaissi et al., 2017). Our results show that this morphology is a result of increased genome and cell size.

Previous work on the brain and nervous system, the skeletal system, and the circulatory and excretory systems in salamanders also revealed distinct patterns of phenotypic change accompanying evolutionary increases in genome and cell size. In the brain, larger and fewer cells impact tissue organization, leading to an increase in gray matter relative to white matter as well as increased cell density (Roth et al., 1990). In addition, slower rates of cell proliferation and migration caused by large genome and cell size result in a decrease in lamination within the tectum mesencephali (Schmidt and Roth, 1993). In the skeletal system, increased genome and cell size (in combination with decreased body size) appears to disrupt skeletal development because the prerequisite tissues that form bones are reduced to significantly fewer cells (Hanken, 1982, 1984; Wake, 1991). In some cases, the carpal and tarsal elements of the feet remain cartilaginous and also fused due to a failure to separate during development (Wake, 1966; Alberch and Alberch, 1981). In the circulatory system, increased genome size is correlated with increased red blood cell size (Villalobos et al., 1988; Mueller et al., 2008) as well as increased capillary diameters (Fig. 6) (Snyder and Sheafor, 1999). In the excretory system, experimental increase in cell size (through induction of polyploidy) altered the morphology and number of cells comprising the pronephric tubules, which are excretory structures similar in morphology to capillaries; however, tubule diameter remained unchanged (Fankhauser, 1945).

Overall, the patterns of phenotypic change that we report in the heart and liver, combined with previous work documenting patterns from the brain, skeleton, circulatory, and excretory systems, suggest that the impact of genome and cell size increase on phenotype is organ specific. This lack of similarity suggests that, for each developing organ, unique relationships exist between genome- and cell-level parameters and the morphological outcome of the developmental system. Because large genome and cell size decreases the rate of development, reduces the number of cells involved in morphogenesis, and/or alters the composition and geometry of tissues, a full understanding of the link between cell size and morphology requires understanding which of these effects is relevant for each organ. More generally, organs that

Table 2. Mean and standard deviation for genome size and morphological traits. $n = 5$ individuals unless otherwise noted; five slides were measured per individual.

		Heart		Liver			
Species	Snout-Vent Length (mm)	Ventricle Volume (mm^3)	Myocardial Area (mm^2)	Liver Volume (mm^3)	Hepatic Tissue Area (mm^2)	Number of Sinusoids	Mean Size of Vascular Structures (mm^2)
Plethodon cinereus	40.1 ± 0.7	0.52 ± 0.06	0.118 ± 0.01	15.9 ± 3.8	0.136 ± 0.01	60 ± 7.1	0.0023 ± 0.0002
P. montanus	49.7 ± 1.1	1.44 ± 0.35	0.101 ± 0.004	33.1 ± 15.9	0.14 ± 0.01	57.1 ± 4.7	0.0024 ± 0.0005
P. cylindraceus	70.4 ± 1.6	3.77 ± 1.24	0.107 ± 0.01	120 ± 72.5	0.123 ± 0.01	58.4 ± 8.8	0.0021 ± 0.0002
P. metcalfi	61.9 ± 4.2	3.74 ± 1.63	0.106 ± 0.004	70.6 ± 41.3	0.136 ± 0.01	54.7 ± 6.6	0.0025 ± 0.0002
P. glutinosus	66.9 ± 2.4	3.71 ± 1.63	0.101 ± 0.002 ($n = 4$)	77.9 ± 40.3	0.127 ± 0.01	59.6 ± 3.5	0.0021 ± 0.0002
P. vehiculum	50.5 ± 0.7	0.9 ± 0.1	0.09 ± 0.004	40 ± 5.6	0.141 ± 0.003	34.4 ± 3.0	0.0041 ± 0.0005
P. dunni	68.7 ± 1.2	5.72 ± 1.59	0.065 ± 0.01	112.1 ± 63.1 ($n = 3$)	0.136 ± 0.004	32.4 ± 4.9	0.0042 ± 0.0002
P. vandykei	54.2 ± 2.0	1.51 ± 0.42	0.073 ± 0.01	62.2 ± 17.9 ($n = 4$)	0.142 ± 0.002	26.3 ± 4.8	0.0054 ± 0.0006
P. idahoensis	58.1 ± 2.1	2.63 ± 0.78	0.043 ± 0.01	40.1 ± 14.7 ($n = 4$)	0.143 ± 0.004	23.5 ± 3.0	0.0061 ± 0.0002

share structural properties (e.g., tubes vs. solid masses of tissue vs. tissue with lacunae) may respond similarly to increases in genome and cell size, allowing predictions from our work to as-yet-unstudied organs (e.g., our results in the liver predict similar effects on sinusoids in the spleen).

PROPOSED GENOME AND CELL SIZE EFFECTS ON HEART DEVELOPMENT

We propose three developmental hypotheses explaining the decrease in ventricular musculature associated with increases in genome and cell size. First, blood flow plays a significant epigenetic role in vertebrate heart development by creating pressure gradients in the developing heart (Santhanakrishnan and Miller, 2011; Johnson et al., 2015). Altering erythrocyte size and morphology can potentially change the fluid dynamics of blood, which in turn would change the degree of pressure in the heart during development (Dupin et al., 2008; AlMomani et al., 2012). Testing this hypothesis would require measuring blood flow, its effects on gene expression, and the morphogenetic outcomes in the developing hearts of salamanders with different genome sizes.

Second, the reduction of ventricle muscle might be the result of slower rates of development and truncation of heart organogenesis at an earlier ontogenetic stage because of large genome and cell size, producing a paedomorphic heart. An ontogenetic study comparing heart morphology in the model salamander *Ambystoma mexicanum* (the axolotl) found that the larval (premetamorphic) heart had significantly less trabeculated myocardia and a lack of internal ridges in the ventricle compared to the postmetamorphic heart (Olejnickova et al., 2021). These results are consistent with the hypothesis that paedomorphosis underlies the negative correlation between trabeculated myocardia and genome size in *Plethodon*. *Plethodon* and *A. mexicanum* do have significant differences in life history and morphology. *Ambystoma mexicanum* typically remain in the aquatic form as sexually mature adults that rely on gills for respiration, but under rare circumstances, they can metamorphose into a terrestrial form that relies on lungs and skin for breathing (Olejnickova et al., 2021). In contrast, *Plethodon* salamanders all undergo direct development (i.e., they lack an aquatic larval stage and metamorphosis, and instead hatch from a terrestrial egg in the form of a tiny adult). In addition, *Plethodon* salamanders are lungless, which was demonstrated to impact heart morphology (Lewis and Hanken, 2017). However, direct development in *Plethodon* recapitulates many of the developmental stages of larval and metamorphic ontogeny inside the egg, and the impacts of lunglessness on heart morphology are largely atrial (Kerney et al., 2011; Lewis and Hanken, 2017). Thus, despite these differences, the *A. mexicanum* results do lend support to the hypothesis of a paedomorphic heart in *Plethodon*.

Table 3. Results from the PGLS linear regressions showing the individual interactions between the predictor and response variables. Significant *P*-values are bolded.

Response Variable	Predictor Variable	*t*	*P*
Liver volume (mm^3)			
	Genome size (Gb)	–0.1	0.959
	Snout-vent length (mm)	7.7	**<0.001**
Hepatic tissue area (mm^2)			
	Genome size (Gb)	4.8	**0.005**
	Snout-vent length (mm)	–5.1	**0.004**
Average vascular structure size (mm^2)			
	Genome size (Gb)	14.1	**<0.001**
	Snout-vent length (mm)	–5.2	**0.004**
Number of vascular structures			
	Genome size (Gb)	–12.8	**<0.001**
	Snout-vent length (mm)	3.8	**0.012**
Ventricle volume (mm^3)			
	Genome size (Gb)	0.1	0.959
	Snout-vent length (mm)	8.0	**<0.001**
Myocardial area (mm^2)			
	Genome size (Gb)	–6.9	**0.001**
	Snout-vent length (mm)	0.7	0.612

Third, morphogenesis and pattern formation can be fundamentally changed when cell size and cell number change (Alberch and Gale, 1985). Because ventricle size was not correlated with cell size, increased cell size must be accompanied by decreased cell numbers. The implications of undergoing heart development with fewer, larger cells are not understood. Testing these latter two hypotheses would require comparative developmental analyses across taxa with different genome and cell sizes to reveal how heart morphogenesis is impacted by changes in developmental rate and in the size and number of cells.

PROPOSED GENOME AND CELL SIZE EFFECTS ON LIVER STRUCTURE

The most prominent change in liver phenotype as genome and cell size increases is related to tissue geometry and vasculature, which includes arteries, veins, and sinusoids. As genome and cell sizes increase, the sizes of the vascular structures also increase—likely to accommodate larger blood cells—whereas the number of vascular structures decreases. Thus, large genome and cell sizes are associated with fewer, larger vascular structures. Liver size is determined by body size in *Plethodon* (Fig. 5), which means that increases in cell size are accompanied by decreases in cell number. We hypothesize that if the number of vascular structures was unchanged, their increased size would likely cause the tissue to become structurally and/or functionally compromised because they would occupy too much space, at the expense of hepatocytes. Therefore, we hypothesize that the number of vascular structures is constrained to maintain organ structural integrity and functionality.

IMPLICATIONS OF MORPHOLOGICAL EVOLUTION ON PERFORMANCE AND FITNESS

The morphological changes that result from increased genome and cell size can have functional consequences. In some cases, functional consequences have been inferred from organs showing patterns of compensatory evolution to offset the negative effects of genome and cell size increase. For example, species with extremely low biological size indices have proportionally larger eyes and regions of the brain—thalamus, pretectum, and midbrain—responsible for visual and visuomotor functions (Roth et al., 1990), as well as a proportional shift in the retina to increase the number of small cones relative to the large rods (Roth et al., 1988, 1990). These changes in brain and eye morphology offset the low number of large neurons, maintaining the acuity required for visual predation (Roth et al., 1990). Similarly, the evolution of wider capillary diameters and enucleated erythrocytes in miniaturized lineages are hypothesized to be compensatory responses that facilitate blood flow with larger erythrocytes (Villalobos et al., 1988; Snyder and Sheafor, 1999; Mueller et al., 2008; Itgen et al., 2019; Decena-Segarra et al., 2020).

We hypothesize that heart and liver functions are affected by the evolutionary changes we report in *Plethodon* as genome and cell size increase. In the heart, the decreased myocardial volume and increased intertrabecular space in the ventricle likely reduce

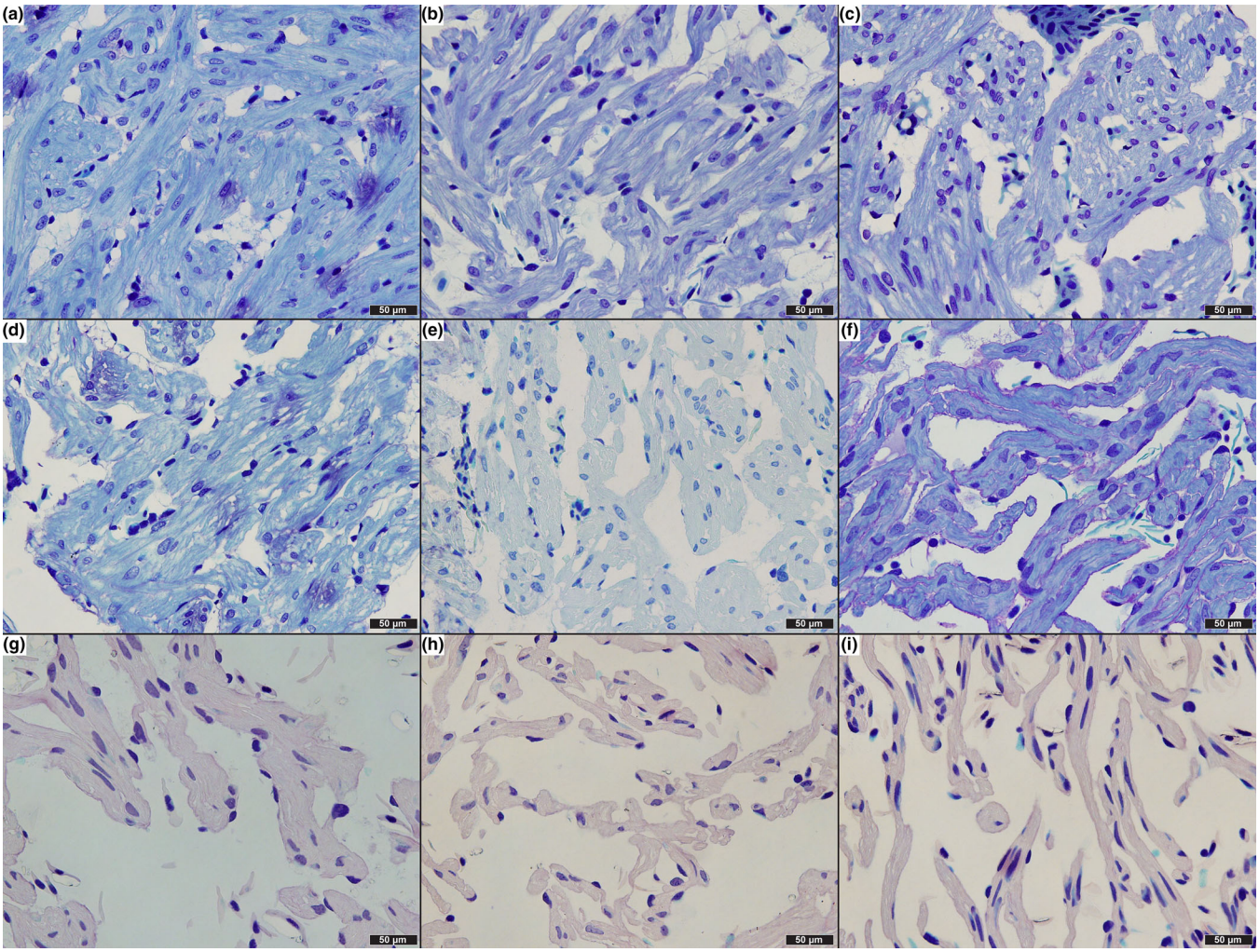

Figure 2. Histological sections of the ventricle at 20× magnification for each species arranged by increasing genome size. (a) *Plethodon cinereus*, 29.3 Gb; (b) *P. montanus*, 36 Gb; (c) *P. cylindraceus*, 37.1 Gb; (d) *P. metcalfi*, 38.3 Gb; (e) *P. glutinosus*, 38.9 Gb; (f) *P. vehiculum*, 46.4 Gb; (g) *P. dunni*, 52.3 Gb; (h) *P. vandykei*, 54.6 Gb; (i) *P. idahoensis*, 67 Gb.

the ventricle's capacity to produce force. Conversely, this reduction in myocardium allows the ventricle to hold greater blood volume. A reduction of force production and increased volume capacity would alter the stroke volume and ejection fraction of the heart. Overall functional measures such as heart rate and cardiac output could be affected as well, although Olejnickova et al. (2021) found no differences in heart rate between larval-stage and postmetamorphic individuals of *A. mexicanum*, despite morphological differences in trabeculated myocardia similar to those we report across *Plethodon*. Trabeculated myocardia also serve a critical role in the electrophysiology of amphibian hearts, and tissue geometry has been linked to signal propagation speed of cultured cardiomyocytes (Kucera et al., 1998; Sedmera et al., 2003). Olejnickova et al. (2021) found that the rate of signal transduction was significantly slower in larval-stage hearts than in postmetamorphic hearts in *A. mexicanum*, but that there were no differences in the activation pattern in the ventricle. These findings suggest that changes in trabeculae morphology associated with genome size could also affect *Plethodon* heart electrophysiology.

In the liver, changes in hepatic tissue organization likely affect function as well. Large genome and cell size impacted the organization of portal triads and the cord-like morphology of hepatocytes, as well as reducing the number of vascular structures. As a result, many hepatocytes do not come into direct contact with any vascular structures, limiting their access to oxygen and nutrient supply and thus impacting their metabolic contribution to overall organ function. Testing this hypothesis would require comparative analyses of liver function across taxa with different genome and cell sizes.

It is important to consider, however, whether these hypothesized cell- and organ-level changes in function, associated with a more-than-doubling of genome size, would have any effect on fitness in salamanders. Variation in morphology is connected to fitness through its effects on organismal performance

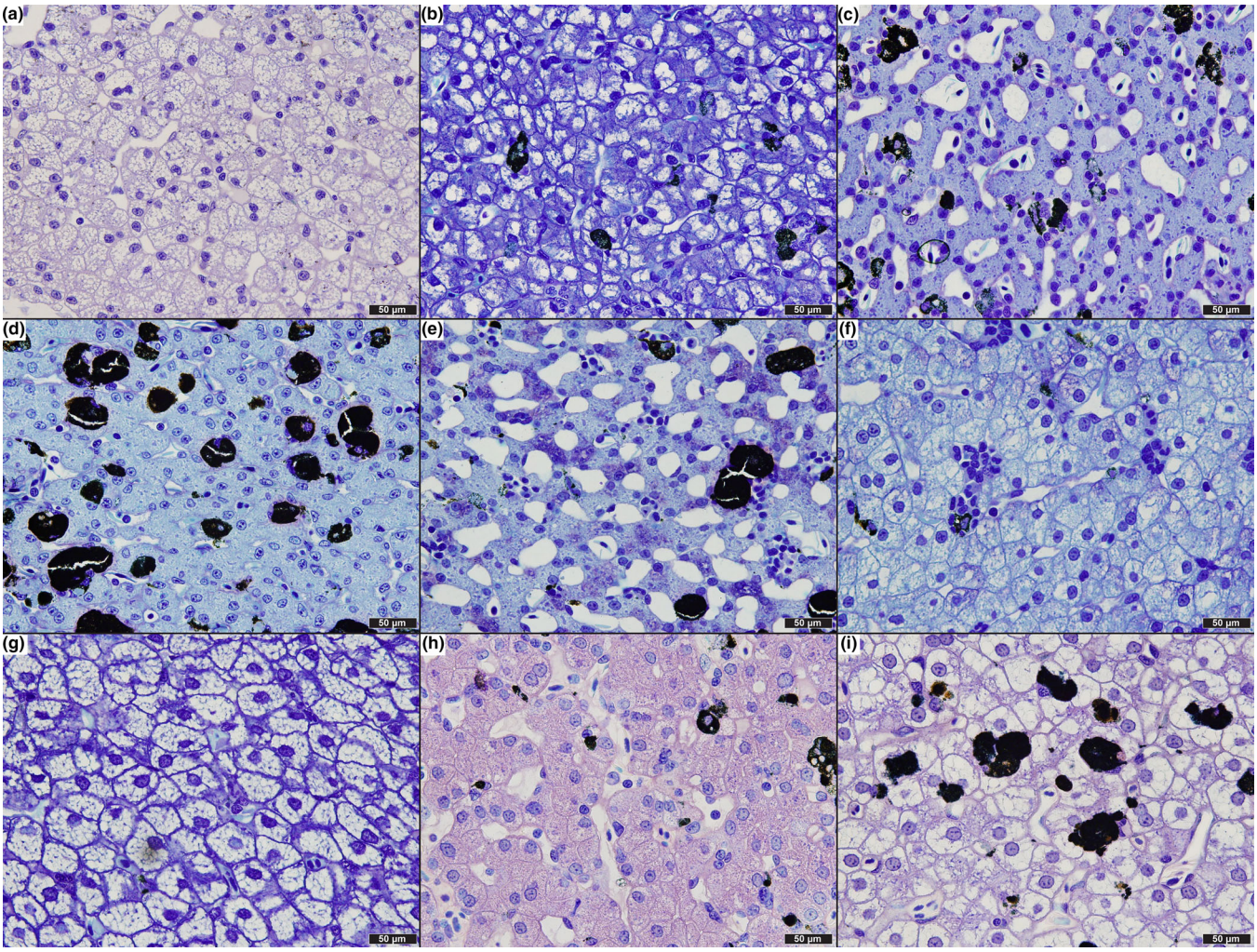

Figure 3. Histological sections of the liver at 20× magnification for each species arranged by increasing genome size. (a) *Plethodon cinereus*, 29.3 Gb; (b) *P. montanus*, 36 Gb; (c) *P. cylindraceus*, 37.1 Gb; (d) *P. metcalfi*, 38.3 Gb; (e) *P. glutinosus*, 38.9 Gb; (f) *P. vehiculum*, 46.4 Gb; (g) *P. dunni*, 52.3 Gb; (h) *P. vandykei*, 54.6 Gb; (i) *P. idahoensis*, 67 Gb.

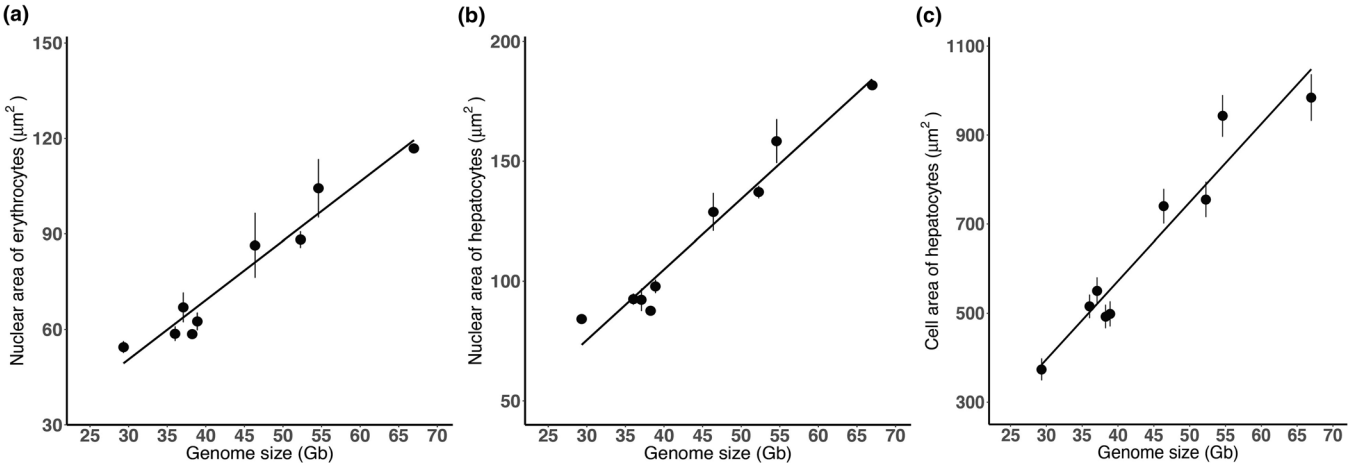

Figure 4. Genome size has a strong positive correlation with the (a) nuclear area of erythrocytes, (b) nuclear area of hepatocytes, and (c) cell area of hepatocytes across the nine species. Trend lines shown for visualization. Error bars represent standard error.

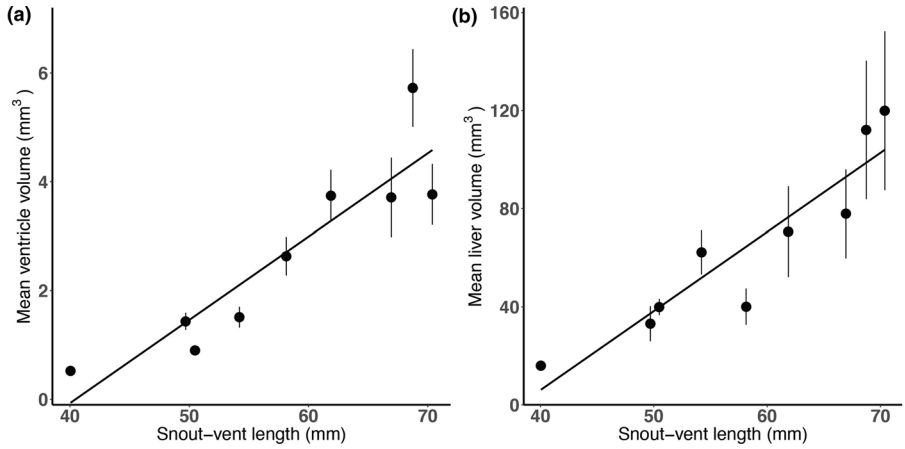

Figure 5. Body size (SVL) is positively correlated with (a) ventricle size and (b) liver size. Trend lines shown for visualization. Error bars represent standard error.

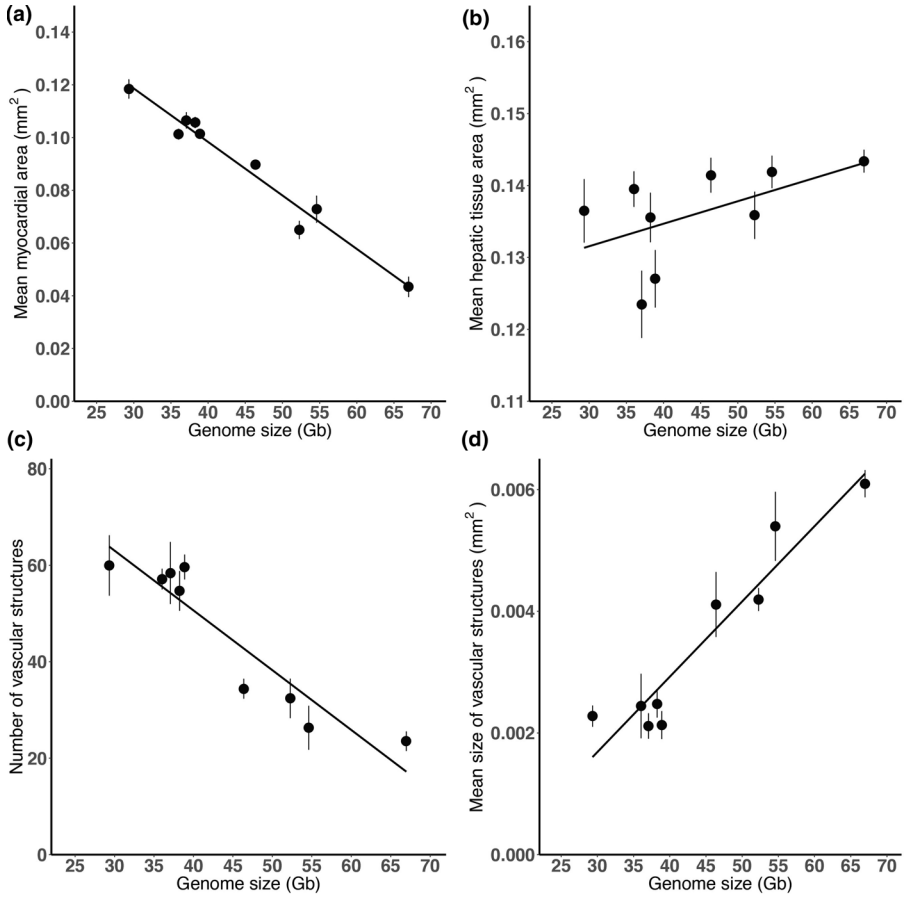

Figure 6. An increase in genome size is correlated with (a) a decrease in myocardial area, (b) an increase in hepatic tissue area, (c) a decrease in the number of vascular structures, and (d) an increase in the size of vascular structures. Trend lines shown for visualization. Error bars represent standard error.

(Arnold, 1983). Morphology can vary without impacting performance, and performance, in turn, can vary without impacting fitness (Bock, 1980). Are the evolutionary changes that we report here in organ structure, and the accompanying changes we hypothesize in organ function, likely to have impacted organismal performance and fitness? We suggest that the answer is no, as a consequence of salamanders' incredibly low metabolic rates (Gatten et al., 1992; Uyeda et al., 2017; Gardner et al.,

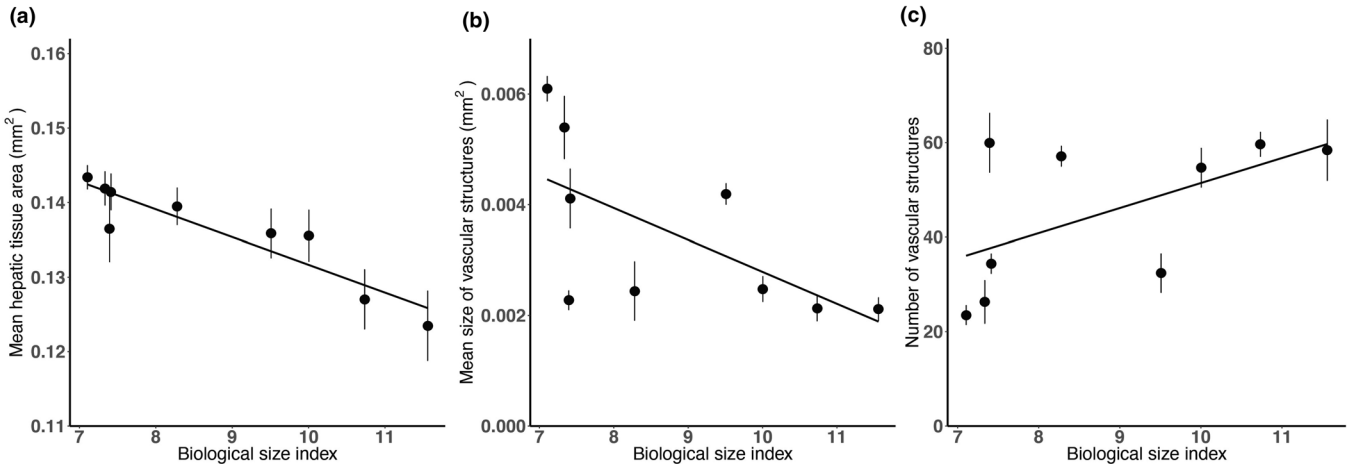

Figure 7. **Biological size index (SVL / $\sqrt{}$ genome size) plotted against (a) hepatic tissue area, (b) the size of vascular structures, and (c) the number of vascular structures. Trend lines shown for visualization. Error bars represent standard error.**

2020; Johnson et al., 2021). More generally, we suggest that low metabolic rates relaxed selective pressure on metabolic organ function, allowing for greater variation in morphology without negatively impacting organismal performance or fitness (and without leading to compensatory evolution). This, in turn, allowed cell size to evolve driven largely by genome-level processes (e.g., transposable element proliferation and deletion; Sun et al., 2012). The range of genome and cell sizes produced throughout the clade's evolutionary history has been funneled through a conserved developmental system, producing a range of morphologies during organogenesis. The "permissive" organismal phenotype of salamanders is thus a powerful tool for examining how the output of developmental systems responds to changes in the fundamental parameter of cell size.

AUTHOR CONTRIBUTIONS

MWI and RLM conceptualized the idea of the study. MWI, DSS, SKS, and RLM designed methodology and curated the data. MWI, GRN, DSS, SKS, and RLM collected the data. MWI, GRN, SKS, and RLM analyzed the data. MWI and RLM wrote the original draft, performed visualization, and acquired funding. MWI, DSS, and RLM reviewed and edited the manuscript. SKS and RLM provided resources. RLM administered the project and performed supervision. All authors contributed to revising the manuscript and have approved the final manuscript.

ACKNOWLEDGMENTS

Specimens of *Ambystoma mexicanum* were obtained from the Ambystoma Genetic Stock Center, which is funded through National Institutes of Health grant: P40-OD019794. We thank A. Summers, the Summers lab, and the Karel Liem Bioimaging Facility at the University of Washington's Friday Harbor Laboratories for allowing us access to their CT scanner and for assistance scanning the specimens. For assistance in the field, we thank A. Cicchino, A. H. Griffing, J. Hayes, M. Hayes, E. Itgen, J. Itgen, F. Rodríguez Vásquez, and S. K. Sessions. For discussion of analyses and the manuscript, we thank members of MWI's dissertation committee K. Hoke, D. Sloan, and W. Zhou. This research was funded by the National Science Foundation (grant 1911585 awarded to RLM), the GREG R.C. Lewontin Early Award awarded to MWI, the Chicago Herpetological Society Grant awarded to MWI, the Stephen and Ruth Wainwright Endowment awarded to MWI, and the Helen T. and Frederick M. Gaige Award awarded to MWI. Animal use was approved by the Institutional Animal Care and Use Committee of Colorado State University and carried out in accordance with protocol 17–7189A.

DATA ARCHIVING

Data used in analyses are deposited on Dryad https://doi.org/10.5061/dryad.6djh9w13b. CT data are available on MorphoSource.org under project ID 000431591.

CONFLICT OF INTEREST

The authors declare no conflict of interest.

REFERENCES

Akat, E., & B. Göçmen. 2014 A histological study of hepatic structure of *Lyciasalamandra arikani* (Urodela: Salamandridae). *Russ. J. Herpetol.* 21:201–204.

Akat, E., & H. Arkan. 2017 A histological study on liver of near eastern fire salamander, *Salamandra infraimmaculata martens*, 1885 (Urodela: Salamandridae). *Acta Zool. Bulg.* 69:317–321.

Akiyoshi, H., & A. M. Inoue. 2012 Comparative histological study of hepatic architecture in the three orders of amphibian livers. *Comp. Hepatol.* 11:1–8.

Alberch, P. 1982. Developmental constraints in evolutionary processes. Pp. 313–332 *in* J. T. Bonner, ed. Evolution and development: Dahlen Konferezen. Springer-Verlag, New York.

Alberch, P. 1983 Morphological variation in the neotropical salamander genus *Bolitoglossa*. *Evolution* 37:906–919.

Alberch, P., & E. Gale. 1985 A developmental analysis of an evolutionary trend: digital reduction in amphibians. *Evolution* 39:8–23.

Alberch, P., & J. Alberch. 1981 Heterochronic mechanisms of morphological diversification and evolutionary change in the neotropical salamander, *Bolitoglossa occidentalis* (Amphibia: Plethodontidae). *J. Morphol.* 167:249–264.

Alberch, P., S. J. Gould, G. F. Oster, & D. B. Wake. 1979 Size and shape in ontogeny and phylogeny. *Paleobiology* 5:296–317.

AlMomani, T. D., S. C. Vigmostad, V. Keshav Chivukula, L. Al-zube, O. Smadi, & S. BaniHani. 2012 Red blood cell flow in the cardiovascular system: a fluid dynamics perspective. *Crit. Rev. Biomed. Eng.* 40:427–440.

Arnold, S. J. 1983 Morphology, performance, and fitness. *Am. Zool.* 23:347–361.

Arnold, S.J. 1992 Constraints on phenotypic evolution. *The American Naturalist*, 140:S85–S107.

Bachmann, K. 1970 Feulgen slope determinations of urodele nuclear DNA amounts. *Histochemie*, 22:289–293.

Baverstock, H., N.S., Jeffery, & S.N., Cobb. 2013 The morphology of the mouse masticatory musculature. *Journal of Anatomy*, 223:46–60.

Benjamini, Y., and Y., Hochberg. 2000 On the adaptive control of the false discovery rate in multiple testing with independent statistics. *Journal of Educational and Behavioral Statistics*, 25:60–83.

Bock, W.J. 1980 The definition and recognition of biological adaptation. *American Zoologist*, 20:217–227.

Brakefield, P.M., V., French, & B.J., Zwaan. 2003 Development and the genetics of evolutionary change within insect species. *Annual Review of Ecology, Evolution, and Systematics*, 34:633–660.

Brakefield, P.M. 2006 Evo-devo and constraints on selection. *Trends in Ecology & Evolution*, 21:362–368.

Chan, C.J., C.P., Heisenberg, & T., Hiiragi. 2017 Coordination of morphogenesis and cell-fate specification in development. *Current Biology*, 27:R1024–R1035.

D'Ario, M., R., Tavares, K., Schiessl, B., Desvoyes, C., Gutierrez, M., Howard, & R., Sablowski. 2021 Cell size controlled in plants using DNA content as an internal scale. *Science*, 372:1176–1181.

Decena-Segarra, L.P., L., Bizjak-Mali, A., Kladnik, S.K., Sessions, & S.M., Rovito. 2020 Miniaturization, genome size, and biological size in a diverse clade of salamanders. *The American Naturalist*, 196:634–648.

Dupin, M.M., I., Halliday, C.M., Care, & L.L., Munn. 2008 Lattice Boltzmann modelling of blood cell dynamics. *International Journal of Computational Fluid Dynamics*, 22:481–492.

Edgar, R.C. 2004 MUSCLE: multiple sequence alignment with high accuracy and high throughput. *Nucleic Acids Research*, 32:1792–1797.

Elias, H., & H., Bengelsdorf. 1952 The structure of the liver of vertebrates. *Acta Anatomica*, 14:297–337.

Fankhauser, G. 1945 The effects of changes in chromosome number on amphibian development. *The Quarterly Review of Biology*, 20:20–78.

Fedorov, A., R., Beichel, J., Kalpathy-Cramer, J., Finet, J.C., Fillion-Robin, S., Pujol, C., Bauer, D., Jennings, F., Fennessy, M., Sonka, J., Buatti, S., Aylward, J.V., Miller, S., Pieper, & R., Kikinis. 2012 3D Slicer as an image computing platform for the Quantitative Imaging Network. *Magnetic Resonance Imaging*, 30:1323–1341.

Gardner, J.D., M., Laurin, & C.L., Organ. 2020 The relationship between genome size and metabolic rate in extant vertebrates. *Philosophical Transactions of the Royal Society B*, 375:20190146.

Gatten, R.E.J., K., Miller, & R.J., Full. 1992 Energetics at rest and during locomotion. Pp. 314–377 in M.E. Feder, ed. Environmental physiology of the amphibians. Univ. of Chicago Press, Chicago.

Gerber, S. 2014 Not all roads can be taken: development induces anisotropic accessibility in morphospace. *Evolution and Development*, 16:373–381.

Gignac, P.M., N.J., Kley, J.A., Clarke, M.W., Colbert, A.C., Morhardt, D., Cerio, I.N., Cost, P.G., Cox, J.D., Daza, C.M., Early, M.S., Echols, R.M., Henkelman, A.N., Herdina, C.M., Holliday, Z., Li, K., Mahlow, S., Merchant, J., Müller, C.P., Orsbon, D.J., Paluh, M.L., Thies, H.P., Tsai, & L.M., Witmer. 2016 Diffusible iodine-based contrast-enhanced computer tomography (diceCT): an emerging tool for rapid, high-resolution, 3-D imaging of metazoan soft tissues. *Journal of Anatomy*, 228:889–909.

Gokhale, R.H., & A.W., Shingleton. 2015 Size control: the developmental physiology of body and organ size regulation. *WIREs Developmental Biology*, 4:335–356.

Gould, S.J. 1985 Ontogeny and phylogeny. Harvard Univ. Press, Cambridge, MA.

Gregory, T.R. 2005 Genome size evolution in animals. Pp. 314–377 in T.R. Gregory, ed. The evolution of the genome. Elsevier, San Diego, CA.

Gregory, T.R. 2021 Animal genome size database. Available via http://www.genomesize.com.

Hanken, J. 1982 Appendicular skeletal morphology in minute salamanders, genus *Thorius* (Amphibia: Plethodontidae): growth regulation, adult size determination, and natural variation. *Journal of Morphology*, 174:57–77.

Hanken, J. 1983 Miniaturization and its effects on cranial morphology in plethodontid salamanders, genus *Thorius* (Amphibia: Plethodontidae): II. The fate of the brain and sense organs and their role in skull morphogenesis and evolution. *Journal of Morphology*, 177:255–268.

Hanken, J. 1984 Miniaturization and its effects on cranial morphology in plethodontid salamanders, genus *Thorius* (Amphibia: Plethodontidae). I. Osteological variation. *Biological Journal of the Linnean Society*, 23:55–75.

Hanken, J., & D.B., Wake. 1993 Miniaturization of body size: organismal consequences and evolutionary significance. *Annual Review of Ecology and Systematics*, 24:501–519.

Hardie, D.C., T.R., Gregory, & P.D.N., Herbert. 2002 From pixels to picograms: a beginners' guide to genome quantification by Feulgen image analysis densitometry. *Journal of Histochemistry and Cytochemistry*, 50:735–749.

Hedrick, B.P., L., Yohe, A., Vander Linden, L.M., Dávalos, K., Sears, A., Sadier, S.J., Rossiter, K.T.J., Davies, & E., Dumont. 2018 Assessing soft-tissue estimates in museum specimens imaged with diffusible iodine-based contrast-enhanced computed tomography (diceCT). *Microscopy and Microanalysis*, 24:284–291.

Highton, R. 1989 Biochemical evolution in the slimy salamanders of the *Plethodon glutinosus* complex in the eastern United States. Part I. Geographical protein variation. *Illinois Biological Monographs*, 57:1–78.

Highton, R. 1995 Speciation in eastern North American salamanders of the genus *Plethodon*. *Annual Review of Ecology and Systematics*, 26:579–600.

Horner, H.A., & H.C., Macgregor. 1983 C value and cell volume: their significance in the evolution and development of amphibians. *Journal of Cell Science*, 63:135–146.

Humason, G.L. 1962 Animal tissue techniques. W. H. Freeman and Company, San Francisco, CA.

Itgen, M.W., P., Prša, R., Janža, L., Skubic, J.H., Townsend, A., Kladnik, L., Bizjak-Mali, & S.K., Sessions. 2019 Genome size diversification in Central American bolitoglossine salamanders (Caudata; Plethodontidae). *Copeia*, 107:560–566.

Jaekel, M., & D.B., Wake. 2007 Developmental processes underlying the evolution of a derived foot morphology in salamanders. *Proceedings of the National Academy of Sciences*, 104:20437–20442.

Johnson, B., D., Bark Jr., I., Van Herck, D., Garrity, & L., Prasad Dasi. 2015 Altered mechanical state in the embryonic heart results in time-dependent decreases in cardiac function. *Biomechanics and Modeling in Mechanobiology*, 14:1379–1389.

Johnson, B.B., J.B., Searle, & J.P., Sparks. 2021 Genome size influences adaptive plasticity of water loss, but not metabolic rate, in lungless salamanders. *Journal of Experimental Biology*, 224:jeb242196.

Kerney, R.R., D.C., Blackburn, H., Müller, & J., Hanken. 2011 Do larval traits re-evolve? Evidence from the embyogenesis of a direct-developing salamander, *Plethodon cinereus*. *Evolution*, 66:252–262.

Keyte, A.L., & K.K., Smith. 2014 Heterochrony and developmental timing mechanisms: changing ontogenies in evolution. *Seminars in Cell and Developmental Biology*, 34:99–107.

Kim, W., & E.H., Jho. 2018 The history and regulatory mechanism of the Hippo pathway. *BMB Reports*, 51:106–118.

Kucera, J.P., A.G., Kléber, & S., Rohr. 1998 Slow conduction in cardiac tissue, II: effects of branching tissue geometry. *Circulation Research*, 83:795–805.

Kumar, S., G., Stecher, & K., Tamura. 2016 MEGA7: molecular evolutionary genetics analysis version 7.0 for bigger datasets. *Molecular Biology and Evolution*, 33:1870–1874.

Lanfear, R., P.B., Frandsen, A.M., Wright, T., Senfeld, & B., Calcott. 2017 Partitionfinder 2: new methods for selecting partitioned models of evolution for molecular and morphological phylogenetic analyses. *Molecular Biology and Evolution*, 34:772–773.

Lewis, Z.R., & J., Hanken. 2017 Convergent evolutionary reduction of atrial septation in lungless salamanders. *Journal of Anatomy*, 230:16–29.

Lewontin, R.C. 1972 The genetic basis of evolutionary change. Columbia Univ. Press, New York.

Linke, R., G., Roth, & B., Rottluff. 1986 Comparative studies on the eye morphology of lungless salamanders, family Plethodontidae, and the effect of miniaturization. *Journal of Morphology*, 189:131–143.

Mallarino, R., P.R., Grant, B.R., Grant, A., Herrel, W.P., Kuo, & A., Abzhanov. 2011 Two developmental modules establish 3D beak-shape variation in Darwin's finches. *Proceedings of the National Academy of Sciences*, 108:4057–4062.

Maroudas-Sacks, Y., & K., Keren. 2021 Mechanical patterning in animal morphogenesis. *Annual Review of Cell and Developmental Biology*, 37:469–493.

Marshall, W.F., K.D., Young, M., Swaffer, E., Wood, P., Nurse, A., Kimura, J., Frankel, J., Wallingford, V., Walbot, X., Qu, & A.H., Roeder. 2012 What determines cell size? *BMC Biology*, 10:1–22.

Maynard Smith, J., R., Burian, S., Kauffman, P., Alberch, J., Campbell, B., Goodwin, R., Lande, D., Raup, & L., Wolpert. 1985 Developmental constraints and evolution. *Quarterly Review of Biology*, 60:265–287.

Mizuno, S., & H.C., Macgregor. 1974 Chromosomes, DNA sequences, and evolution in salamanders of the genus *Plethodon*. *Chromosoma*, 48:239–296.

Mueller, R.L., T.R., Gregory, S.M., Gregory, A., Hsieh, & J.L., Boore. 2008 Genome size, cell size, and the evolution of enucleated erythrocytes in attenuate salamanders. *Zoology*, 111:218–230.

Mueller, R.L., C.E., Cressler, R.S., Schwarz, R.A., Chong, & M.A., Butler. 2021 Metamorphosis imposes variable constraints on genome expansion. bioRxiv. https://doi.org/10.1101/2021.05.05.442795.

Newman, C.E., T.R., Gregory, & C.C., Austin. 2016 The dynamic evolutionary history of genome size in North American woodland salamanders. *Genome*, 60:285–292.

Olejnickova, V., H., Kolesova, M., Bartos, D., Sedmera, & M., Gregorovicova. 2021 The tale-tell heart: evolutionary tetrapod shift from aquatic to terrestrial life-style reflected in heart changes in axolotl (*Ambystoma mexicanum*). *Developmental Dynamics*, 250:1–11.

Orne, D., R., Freckleton, G., Thomas, T., Petzoldt, S., Fritz, N., Isaac, & W., Pearse. 2013 caper: comparative analyses of phylogenetics and evolution in R. R package, version 0.5.2.

Oster, G.F., & P., Alberch. 1982 Evolution and bifurcation of developmental programs. *Evolution*, 36:444–462.

Oster, G., N., Shubin, J.D., Murray, & P., Alberch. 1988 Evolution and morphogenetic rules: the shape of the vertebrate limb in ontogeny and phylogeny. *Evolution*, 42:862–884.

Pinheiro, J., D., Bates, S., DebRoy, D., Sarkar, and the R Development Core Team. 2021 nlme: linear and nonlinear mixed effects models. R package, version 3.1.

Powder, K.E., K., Milch, G., Asselin, & R.C., Albertson. 2015 Constraint and diversification of developmental trajectories in cichlid facial morphologies. *EvoDevo*, 6:https://doi.org/10.1186/s13227-015-0020-8.

R Core Team. 2016 R: a language and environment for statistical computing. R Foundation for Statistical Computing, Vienna. Available via http://www.R-project.org/.

Revell, L.J. 2012 Phytools: an R package for phylogenetic comparative biology (and other things). *Methods in Ecology and Evolution*, 3:217–223.

Ronquist, F., M., Teslenko, P., van der Mark, D.L., Ayres, A., Darling, S., Höhna, B., Larget, L., Liu, M.A., Suchard, & J.P., Huelsenbeck. 2012 MrBayes 3.2: efficient Bayesian phylogenetic inference and model choice across a large model space. *Systematic Biology*, 61:539–542.

Roth, G., B., Rottluff, & R., Linke. 1988 Miniaturization, genome size and the origin of functional constraints in the visual system of salamanders. *Naturwissenschaften*, 75:297–304.

Roth, G., B., Rottluff, W., Grunwald, J., Hanken, & R., Linke. 1990 Miniaturization in plethodontid salamanders (Caudata: Plethodontidae) and its consequences for the brain and visual system. *Biological Journal of the Linnean Society*, 40:165–190.

Roth, G., K.C., Nishikawa, C., Naujoks-Manteuffel, A., Schmidt, & D.B., Wake. 1993 Paedomorphosis and simplification in the nervous system of salamanders. *Brain, Behavior, and Evolution*, 42:137–170.

Roth, G., J., Blanke, & D.B., Wake. 1994 Cell size predicts morphological complexity in the brains of frogs and salamanders. *Proceedings of the National Academy of Sciences*, 91:4796–4800.

Roth, G., & W., Walkowiak. 2015 The influence of genome and cell size on brain morphology in amphibians. *Cold Spring Harbor Perspectives in Biology* 7:a019075.

Salazar-Ciudad, I. 2006 Developmental constraints vs. variation properties: how pattern formation can help to understand evolution and development. *Journal of Experimental Zoology Part B: Molecular and Developmental Evolution*, 306:107–125.

Santhanakrishnan, A., & L.A., Miller. 2011 Fluid dynamics of heart development. *Cell Biochemistry and Biophysics*, 61:1–22.

Schmidt, A., & G., Roth. 1993 Patterns of cellular proliferation and migration in the developing tectum mesencephali of the frog *Rana temporaria* and the salamander *Pleurodeles waltl*. *Cell and Tissue Research*, 272:273–287.

Schneider, C.A., W.S., Rasband, & K.W., Eliceiri. 2012 NIH Image to ImageJ: 25 years of image analysis. *Nature Methods*, 9:671–675.

Sedmera, D., M., Reckova, A., deAlmeida, M., Sedmerova, M., Biermann, J., Volejnik, A., Sarre, E., Raddatz, R.A., McCarthy, R.G., Gourdie, & R.P., Thompson. 2003 Functional and morphological evidence for a ventricular conduction system in zebrafish and *Xenopus* hearts. *American Journal of Physiology – Heart and Circulatory Physiology* 284:H1152–H1160.

Sessions, S.K. 2008 Evolutionary cytogenetics in salamanders. *Chromosome Research*, 16:183–201.

Sessions, S.K., & A., Larson. 1987 Developmental correlates of genome size in plethodontid salamanders and their implications for genome evolution. *Evolution*, 41:1239–1251.

Sessions, S.K., & D.B., Wake. 2021 Forever young: linking regeneration and genome size in salamanders. *Developmental Dynamics*, 250:768–778.

Snyder, G.K., & B.A., Sheafor. 1999 Red blood cells: centerpiece in the evolution of vertebrate circulatory system. *American Zoologist*, 39:189–198.

Stephenson, A., J.W., Adams, & M., Vaccarezza. 2017 The vertebrate heart: an evolutionary perspective. *Journal of Anatomy*, 231:787–797.

Sun, C., D.B., Shepard, R.A., Chong, J.L., Arriaza, K., Hall, TA., Castoe, C., Feschotte, D.D., Pollock, & R.L., Mueller. 2012 LTR retrotransposons contribute to genomic gigantism in plethodontid salamanders. *Genome Biology and Evolution*, 4:168–183.

Uller, T., A.P., Moczek, R.A., Watson, P.M., Brakefield, & K.N., Laland. 2018 Developmental bias and evolution: a regulatory network perspective. *Genetics*, 209:949–966.

Uyeda, J.C., M.W., Pennell, E.T., Miller, R., Maia, & C.R., McClain. 2017 The evolution of energetic scaling across the vertebrate tree of life. *The American Naturalist*, 190:185–199.

Vaissi, S., P., Parto, & M., Sharifi. 2017 Anatomical and histological study of the liver and pancreas of two closely related mountain newts: *Neurergus microspilotus* and *N. kaiseri* (Amphibia: Caudata: Salamandridae). *Zoologia*, 34:1–8.

Vickerton, P., J., Jarvis, & N., Jeffery. 2013 Concentration-dependent specimen shrinkage in iodine-enhanced microCT. *Journal of Anatomy*, 223:185–193.

Villalobos, M., P., León, S.K., Sessions, & J., Kezer. 1988 Enucleated erythrocytes in plethodontid salamanders. *Herpetologica*, 44:243–250.

Vinogradov, A.E. 1999 Genome in toto. *Genome*, 42:361–362.

Wagner, A. 2011 Genotype networks shed light on evolutionary constraints. *Trends in Ecology and Evolution*, 26:577–584.

Wake, D.B. 1966 Comparative osteology and evolution of the lungless salamanders, family Plethodontidae. *Southern California Academy of Sciences*, 4:1–111.

Wake, D.B. 1991 Homoplasy: the result of natural selection or evidence of design limitations? *Am. Nat.*, 138:543–567.

Womack, M.C., M.J., Metz, & K.L., Hoke. 2019 Larger genomes linked to slower development and loss of late-developing traits. *The American Naturalist*, 194:854–864.

Revell, L.J. 2010 Phylogenetic signal and linear regression on species data. *Methods in Ecology and Evolution*, 1:319–329.

Associate Editor: T. Kohlsdorf
Handling Editor: M. L. Zelditch

Supporting Information

Additional supporting information may be found online in the Supporting Information section at the end of the article.

Supplementary information